MEDICAL SCIENCE MONITOR

LAB/IN VITRO RESEARCH

e-ISSN 1643-3750
© Med Sci Monit, 2017; 23: 3981-3988
DOI: 10.12659/MSM.897542

Received: 2016.01.12
Accepted: 2016.07.13
Published: 2017.08.17

Role of MicroRNA-93 I in Pathogenesis of Left Ventricular Remodeling via Targeting Cyclin-D1

Authors' Contribution:
Study Design A
Data Collection B
Statistical Analysis C
Data Interpretation D
Manuscript Preparation E
Literature Search F
Funds Collection G

BCDEF 1 Jingjing Zhang*
BCF 1 Li Qin*
ABCDEFG 1 Ling Han
BDF 2 Ying Zhao
CEF 3 Hongfeng Jing
ADEF 4 Wei Song
BEF 1 Haili Shi

1 Department of Cardiology, Central Hospital of Zhengzhou University, Zhengzhou, Henan, P.R. China
2 Department of Cardiology, No. 1 Affiliated Hospital of Zhengzhou University, Zhengzhou, Henan, P.R. China
3 Department of Radiology, Central Hospital of Zhengzhou University, Zhengzhou, Henan, P.R. China
4 Department of Pathology, Affiliated Tumor Hospital of Zhengzhou University, Zhengzhou, Henan, P.R. China

* Jingjing Zhang and Li Qin contributed to the study equally

Corresponding Author: Ling Han, e-mail: ep5699@sina.com
Source of support: Departmental sources

Background: The objective of this study was to identify the pathway responsible for ventricular remodeling.

Material/Methods: We collected remodeling myocardium tissue (n=18) and control myocardium tissue (n=22), and detected the expression of 4 miRNAs in these 2 groups using real-time PCR. We then searched the miRNA database online to find the candidate genes of miR-93. Real-time PCR and Western blot analysis were used to confirm the regulatory relationship.

Results: We found that only miR-93 was decreased in remodeling myocardium tissue, and validated CCND1 to be the direct target gene of miR-93, with the "seed sequence" located within the 3'-UTR of the target gene via luciferase reporter assay system. Furthermore, we established the negative regulatory relationship between miR-93 and CCND1 by determining the relative luciferase activity of cells transfected with wild-type or mutant 3'-UTR of CCND1. We also found that The CCND1 protein and mRNA expression level of HL-1 cells treated with 50 nM miR-93 mimics were apparently lower than the scramble control, and those of the cells treated with 100 nM miR-93 mimics and CCND1 siRNA (100 nM) were even lower than those in the 50 nM treatment group. Meanwhile, cells transfected with miR-93 mimics (50 nM) showed evidently downregulated viability when compared with the scramble controls, while cells transfected with (100 nM) and CCND1 siRNA (100nM) showed even lower viability.

Conclusions: We showed that CCND1 is a direct target of miR-93, and the dysregulation of the miR-93/CCND1 signaling pathway is responsible for the development of ventricular remodeling.

MeSH Keywords: Cell Cycle • Cell Proliferation • MicroRNAs • Ventricular Remodeling

Full-text PDF: https://www.medscimonit.com/abstract/index/idArt/897542

2743 1 7 32

Indexed in: [Current Contents/Clinical Medicine] [SCI Expanded] [ISI Alerting System] [ISI Journals Master List] [Index Medicus/MEDLINE] [EMBASE/Excerpta Medica] [Chemical Abstracts/CAS] [Index Copernicus]

Background

Left ventricular hypertrophy (LVH) develops in 15% to 20% of patients with hypertension. LVR is associated with elevated risk of mortality and morbidity independent of other risk factors, and it remains largely unknown in our understanding of how risk factors lead to adaptive changes in ventricular hypertrophy [1]. It has been reported that in hypertensive individuals, hemodynamic burden contributed 10% to 30% of mass variability to LVH, and more and more studies are being focused on the roles of other factors in cardiac hypertrophy pathogenesis [2–4].

Ventricular remodeling is characterized by changes in function, shape, and size of the heart in response to increased load or cardiac injury, and has a close relationship with the progression and development of heart failure. Numerous risk factors (e.g., neurohumoral activation, hemodynamic load, oxidative stress, nitric oxide production, cytokines, and endothelin) affect the pathogenesis of ventricular remodeling [5]. Dysregulated control of the cell cycle, which is precisely regulated by various biological factors, plays an important part in the pathogenesis of ventricular remodeling [6,7]. A previous study indicated that dysregulated cell cycle progression of cardiomyocytes played a role in left ventricle remodeling and dysfunction in dilated cardiomyopathy [8]. Another study demonstrated that abnormal proliferation of cardiomyocytes is closely related with early symptomatic postinfarction heart failure and LVR [9].

Accumulating evidence shows that microRNAs (miRNAs) can serve as potential therapeutic targets and diagnostic biomarkers [10], but the relationship between heart remodeling and miRNAs has not been identified. A significant association has been identified between heart diseases (e.g., cardiac arrhythmia, myocardial infarction, and cardiac hypertrophy) and miRNAs, indicating that miRNAs participate in the pathogenesis of those medical conditions [11]. A previous miRNA microarray study identified differentially expressed miRNAs between the sample harvested from patients with LVH and normal controls [12], and several miRNAs that were reported to be differentially expressed (e.g., miR -34a, miR-28, miR-148, and miR-93) were selected as candidate miRNAs for subsequent functional analysis. Furthermore, we found miR-93 is differentially expressed and identified CCND1, which has been reported to be involved in the pathogenesis of LVH as a target of miR-93, and explored the role of miR-93/CCND1 in the development of ventricular remodeling. The objective of this study was to identify the role of miR-93 and its target, CCND1, in the pathogenesis of development of LVH.

Material and Methods

Ethics statement

The study protocol was approved by the Research Ethics Committee of our hospital and written consent was obtained from each participant.

Patient samples

We recruited 18 hypertensive patients with LVH (age 46.45±6.68 and M/F: 11/7) and 22 hypertensive patients without LVH (age 47.39±7.83 and M/F: 17/5) at our hospital. The tip of the right atrial appendage was dissected as part of the general surgical procedure in each patient undergoing valve replacement or open-heart surgery for bypass grafting. The characteristics of the participants are summarized in Table 1. The samples were frozen in liquid nitrogen immediately after collection.

Table 1. The characteristics of the participants of this study.

Variable	Hypertension with LVH (n=18)	Hypertension without LVH (n=22)	P value
Age	46.45±6.68	47.39±7.83	NS
Gender			
Male	11	17	NS
Female	7	5	
Surgery			NS
Valve replacement	10	13	
Bypass grafting	8	9	
Ejection fraction	42.34±5.34	43.54±6.21	NS

NS – not significant.

Indexed in: [Current Contents/Clinical Medicine] [SCI Expanded] [ISI Alerting System] [ISI Journals Master List] [Index Medicus/MEDLINE] [EMBASE/Excerpta Medica] [Chemical Abstracts/CAS] [Index Copernicus]

Western blot analysis

Cells were washed twice with PBS and lysed in CelLytic™ MT Cell Lysis Reagent and protease inhibitor cocktail (Sigma-Aldrich, St. Louis, MO) for 15 min on a shaker. After centrifuging at 13 000 rpm for 10 min, the cell lysate was assessed for the protein levels of P-gp and HIPK2. Equal amounts of protein extracts were loaded on 8% SDS–PAGE gels and electrophoresed. After transferring onto nitrocellulose membranes, we blocked the blots with 5% skimmed milk in TBST containing 0.1% Tween-20 for 2 h. Subsequently, the membranes were incubated in anti-CCND1 (Calbiochem, San Diego, CA), and anti-β-actin (Santa Cruz Biotechnology, CA). All primary antibodies were diluted according to the manufacturer's recommendations and the membranes were incubated overnight at 4°C. After washing with TBST, the membranes were incubated for 2 h with horseradish peroxidase (HRP)-conjugated goat anti-mouse or rabbit secondary antibody (Santa Cruz Biotechnology, CA). Protein expression levels were visualized on enhanced chemiluminescence film (Pierce, USA). The Quantity One software was used to quantify protein band intensities. Each experiment was performed 3 times with consistent results.

RNA isolation and real-time PCR

Total RNA from tissue and culture cells was extracted with Trizol (Invitrogen, CA) according to the manufacturer's protocol. cDNA was synthesized with Super Script III reverse transcriptase, oligo(dT), and random primers (Invitrogen, USA). Real-time PCR was performed for the synthesized cDNA to quantify microRNA-1001 expression using TaqMan fluorescence methods. The relative expression of microRNA-93 and CCND1 mRNA is shown as fold difference relative to glyceraldehyde 3-phosphate dehydrogenase (GAPDH).

Cell proliferation assay

MTT assay was used to estimate cell viability. Briefly, HL-1 cells were transfected with either miR-93 or scramble control. After 24-h transfection, cells were seeded into 96-well plates at 5.0×10^3 cells/ml and cultured for 48 h, then 10 µl MTT reagent (5 mg/ml, Sigma) was added to each well and incubated for 4 h at 37°C. The supernatant was removed and 200 µl DMSO (Invitrogen) was added to dissolve the formazan crystals for 30 min. Spectrometric absorbance at a wavelength of 570 nm was measured using a microplate reader (Spectra Max M5, MD). Cells in the control group were considered 100% viable. Each sample was tested in triplicate and all experiments were performed 3 times.

Luciferase assay

CCND1 3'UTR were amplified and subcloned into a pGL3 vector, and the accuracy of the insert was confirmed through direct sequencing. Mutations were introduced into the corresponding position using site-directed mutagenesis. HL-1 cells were cotransfected with the pGL3 vectors containing the 3'-UTR of CCND1 and miR-93 mimics or the miRNA control using Lipofectamine 2000. Luciferase activity was measured 36 h after transfection using the Dual-Luciferase Reporter Assay System (Promega) according to the manufacturer's instructions. The firefly luciferase activity was then normalized to the Renilla luciferase activity. All experiments were performed in triplicate.

Cells culture and transfection

HL-1 cells were purchased from ATCC and cultured in Dulbecco's modified Eagle's medium supplemented with 10% serum. miR-93 mimics and inhibitors and CCND1 siRNA were purchased from Ambion (Austin, TX). Transfection was performed using Lipofectamine 2000.

Cell cycle analysis

Flow cytometry analysis was performed to determine the fraction of G0/G1, S, and G2/M phases of HL-1 cells. Briefly, the cells were transfected with miR-93 mimics or its inhibitor, or CCND1 siRNA, and then harvested by trypsinization. Cold 75% ethanol was used to fix cells overnight at 4°C, followed by washing in PBS 3 times. Next, 10 ul of RNaseA was added and mixed, and then 30 ul of PI (propidium iodide) was added and incubated for 30 min at 37°C, and then loaded onto a flow cytometry device (Beckman Coulter).

Statistical analysis

We used the one-way ANOVA or *t* test, as appropriate, to evaluate differences of the miRNAs and mRNA expression levels between groups. The Wilcoxon rank test was used to evaluate the difference when the data were not in normal distribution. The data are expressed as mean ± standard deviation (SD). The statistical analysis was performed using SPSS 20.0 version (IBM Inc, Chicago, IL). $P<0.05$ was considered to be statistically significant.

Results

MiR-93 is downregulated in remodeling myocardium tissue

In this study, remodeling myocardium tissue (n=18) and control myocardium tissue (n=22) were collected prior to our research, and total RNA from these tissue samples was extracted with Trizol (Invitrogen, CA) according to the manufacturer's protocol. We detected the expression of the 4 miRNAs in these 2 groups using real-time PCR, and found only the expression

Indexed in: [Current Contents/Clinical Medicine] [SCI Expanded] [ISI Alerting System] [ISI Journals Master List] [Index Medicus/MEDLINE] [EMBASE/Excerpta Medica] [Chemical Abstracts/CAS] [Index Copernicus]

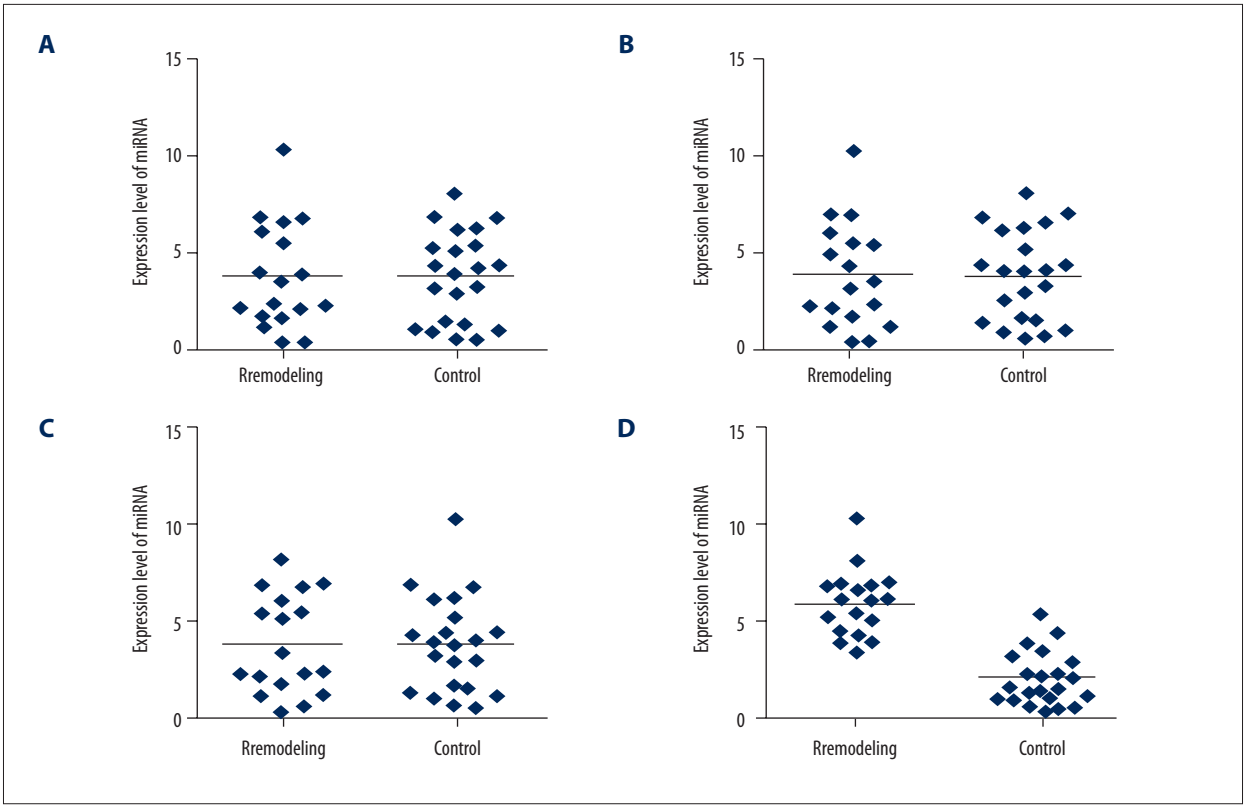

Figure 1. The screening of candidate miRNAs by comparison between expression level in LVH and control. Among miR-34a, miR-28, miR-148, and miR-93, only miR-93 was significantly different between remodeling myocardium tissue and control.

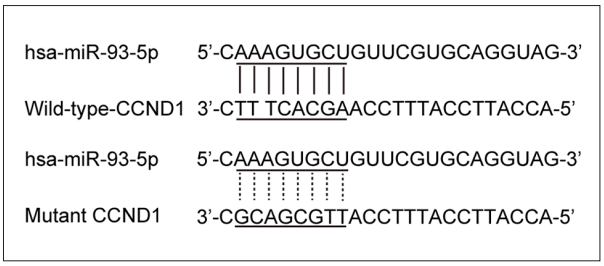

Figure 2. CCND1 as the candidate target gene of miR-93 in HL-1 cells with the 'seed sequence' in the 3'UTR.

level of miR-93 was different in the remodeling myocardium tissue, while the others were comparable with control myocardium tissue (Figure 1).

CCND1 was virtual target of miR-93

We then searched miRanda for the potential target genes to identify the mediators of miR-93. By screening the candidate genes that came out based on their functions, we identified CCND1 was the candidate target gene of miR-93 in remodeling myocardium tissue with the 'seed sequence' in the 3'UTR (Figure 2). We found that only the expression level of CCND1 mRNA and protein were upregulated in the remodeling myocardium tissue compared to those in control myocardium tissue (Figure 3). To further validate the regulatory relationship between miR-93 and CCND1, we also carried out luciferase activity reporter assay in HL-1 cells by transfecting with miR-93 mimics and wild-type or mutant CCND1 3'UTR. As shown in Figure 4, only the luciferase activity from the cells cotransfected with miR-93 and wild-type CCND1 3'UTR were significantly suppressed compared with scramble control (Figure 4), while cells cotransfected with miR-93 and mutant CCND1 3'UTR had substantially abolished inhibition (Figure 4). The results confirmed that CCND1 was a validated target of miR-93 in HL-1 cells. To further define the modulatory relationship between miR-93 and CCND1, we then analyzed the correlation between the expression level of miR-93 and CCND1 mRNA in the tissues (n=40), showing a negative regulatory relationship between miR-93 and CCND1 (Figure 5).

Determination of expression patterns of miR-93 and CCND1 in tissues from different groups

To further validate the hypothesis of the negative regulatory relationship between miR-93 and CCND1, we investigated the mRNA/protein expression level of CCND1 of HL-1 cells transfected with scramble control, different concentrations of miR-93 mimics (50 nM and 100 nM), and CCND1 siRNA (100 nM). As shown in Figure 6, the CCND1 protein (upper panel) and

Indexed in: [Current Contents/Clinical Medicine] [SCI Expanded] [ISI Alerting System] [ISI Journals Master List] [Index Medicus/MEDLINE] [EMBASE/Excerpta Medica] [Chemical Abstracts/CAS] [Index Copernicus]

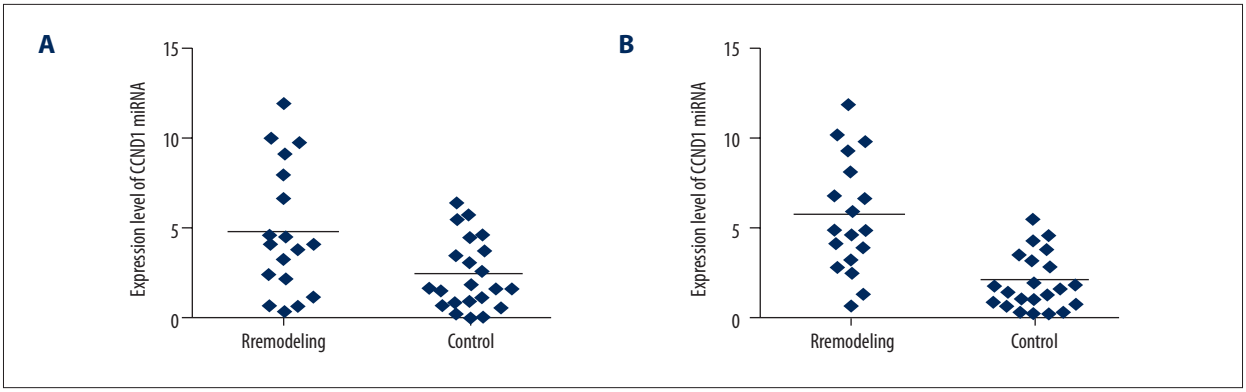

Figure 3. Determination of expression of CCND1 between LVH and control. CCND1 protein (**A**) and mRNA (**B**) were upregulated in the remodeling myocardium tissue compared with control.

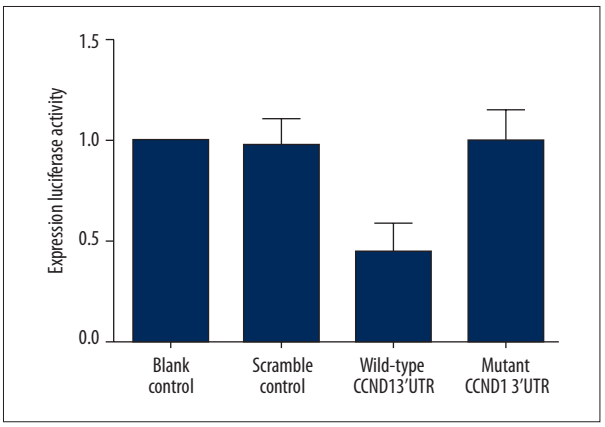

Figure 4. Luciferase activity reporter assay was conducted to verify CCND1 as the direct target gene of miR-93.

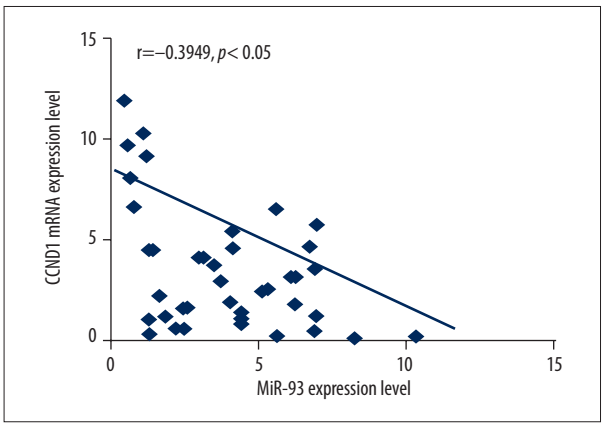

Figure 5. Correlation between the expression level of miR-93 and CCND1 mRNA in remodeling myocardium tissue (n=18) and control (n=22).

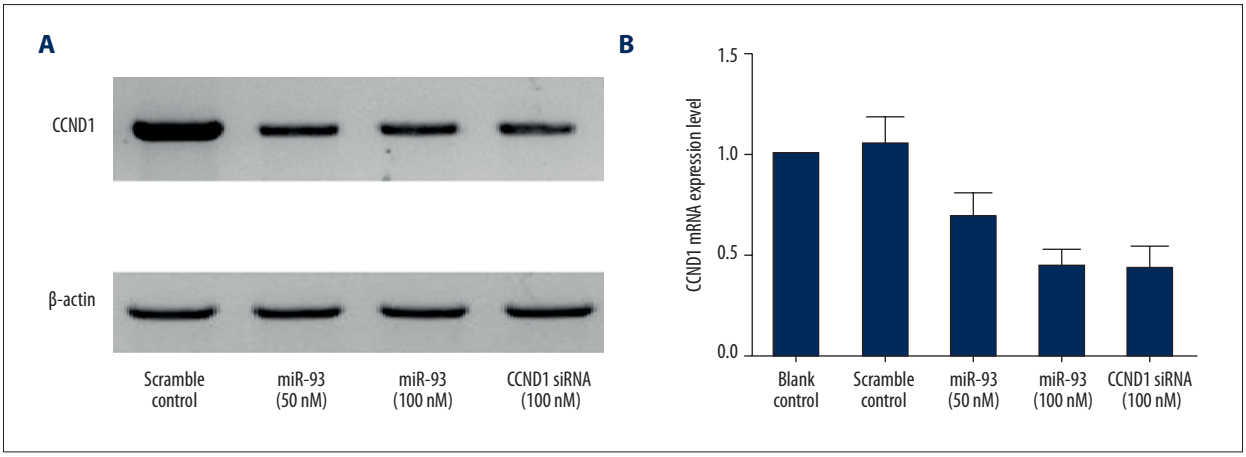

Figure 6. The effects of miR-93 mimics and CCND1 siRNA on the expression of CCND1. The CCND1 protein (**A**) and mRNA expression level (**B**) of HL-1 cells treated with 50 nM miR-93 mimics were apparently lower than in the scramble control, and those of the cells treated with 100 nM miR-93 mimics and CCND1 siRNA (100 nM) were even lower than in the 50 nM treatment group.

Indexed in: [Current Contents/Clinical Medicine] [SCI Expanded] [ISI Alerting System] [ISI Journals Master List] [Index Medicus/MEDLINE] [EMBASE/Excerpta Medica] [Chemical Abstracts/CAS] [Index Copernicus]

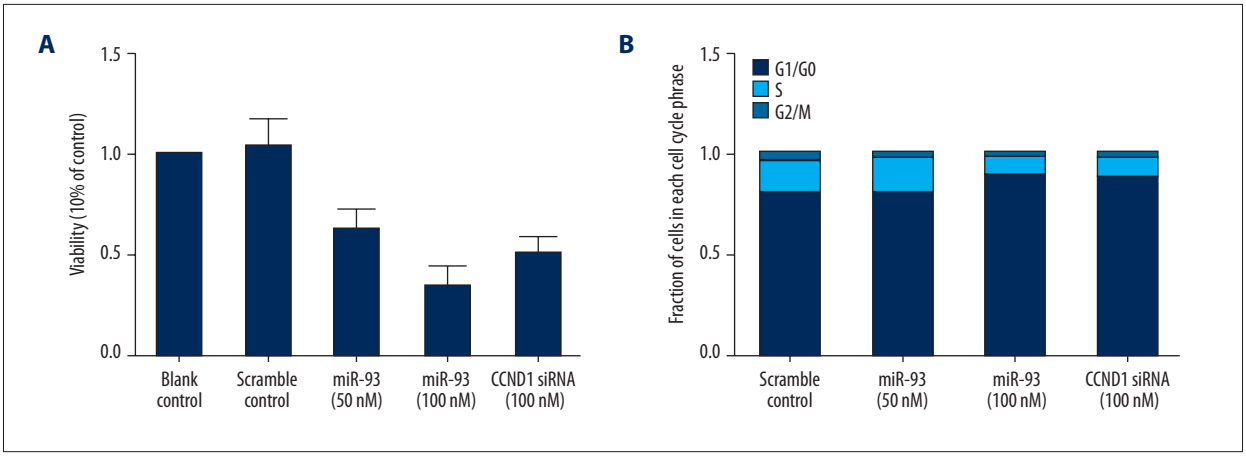

Figure 7. Effect of alternation of miR-93 and CCND1 on the viability and cell cycle of HL-1. (**A**) Cells transfected with miR-93 mimics (50 nM) showed evidently downregulated viability when compared with the scramble controls, while cells transfected with (100 nM) and CCND1 siRNA (100 nM) showed even lower viability. (**B**) The G1 phase percentage of HL-1 transfected with miR-93 mimics (50 nM), miR-93 mimics (100 nM), and CCND1 siRNA (100 nM) was increased from 80% to 85% (miR-93 mimics [50 nM]), 80% to 89% (miR-93 mimics [100 nM]), and 80% to 88% (CCND1 siRNA [100 nM]), respectively, whereas the cells at the S phase decreased from 15% to 13% (miR-93 mimics [50 nM]), 15% to 9% (miR-93 mimics [100 nM]), and 15% to 10% (CCND1 siRNA [100 nM]), and the population of cells at the G2 phase decreased from 5% to 2% (miR-93 mimics [50 nM]), 5% to 2% (miR-93 mimics [100 nM]), and 5% to 2% (CCND1 siRNA [100 nM]), respectively.

mRNA expression level (lower panel) of HL-1 cells treated with 50nM miR-93 mimics were clearly lower than the scramble control, and those of the cells treated with 100 nM miR-93 mimics and CCND1 siRNA (100 nM) were even lower than in the 50 nM treatment group, indicating a concentration-dependent effect of miR-93 on the expression of CCND1, and confirming that miR-93 suppressed the expression of CCND1.

MiR-93 and CCND1 interfered with the viability in HL-1 cells

HL-1 cells were transfected with different concentrations of miR-93 mimics and CCND1 siRNA to further investigate the influence of miR-93 on cell behaviors using MTT assay. As shown in Figure 7, the viability of cells transfected with miR-93 mimics (50 nM) was evidently downregulated (Figure 7A) compared with the scramble controls, while cells transfected with miR-93 mimics (100 nM) and CCND1 siRNA (100 nM) showed even lower viability, indicating that miR-93 negatively regulated the viability of HL-1 cells, while CCND1 positively regulated the viability of HL-1 cells.

miR-93 and CCND1 interfered with cells proliferation in HL-1 cells

To investigate the mechanism underlying the effect of miR-93 and CCND1 on cell proliferation, we carried out cell cycle distribution analysis in HL-1 cells using flow cytometry. The data revealed that overexpression of miR-93 slowed the growth of HL-1 cells in G1 phase, with a decrease proportion of G2/M and S phase cells, as shown in Figure 7B. The results show that, compared with the control group, the G1 phase percentage of HL-1 transfected with miR-93 mimics (50 nM), miR-93 mimics (100 nM), and CCND1 siRNA (100 nM) was increased from 80% to 85% (miR-93 mimics [50 nM]), 80% to 89% (miR-93 mimics [100 nM]), and 80% to 88% (CCND1 siRNA [100 nM]), respectively; whereas the cells at the S phase decreased from 15% to 13% (miR-93 mimics [50 nM]), 15% to 9% (miR-93 mimics [100 nM]), and 15% to 10% (CCND1 siRNA [100 nM]); and the population of cells at the G2 phase decreased from 5% to 2% (miR-93 mimics [50nM]), 5% to 2% (miR-93 mimics [100 nM]), and 5% to 2% (CCND1 siRNA [100 nM]), respectively (Figure 7B). These data demonstrate that overexpression of miR-93 and CCND1 can suppress the proliferation of HL-1 cells by arresting cell growth in G1 phase.

Discussion

Repression of genes coding proteins that influence cardiac structure and contractility lead to cardiac remodeling in response to stress. As novel remodeling hypotheses cannot explain the basic mechanisms of this disorder, another theory of regulation mediated by stress-responsive miRs is put forward. Since it was first discovered in 1993, the role of miRs in cell apoptosis, proliferation, differentiation, and stress responses has been illustrated. However, the role of miRs in heart failure, LVH, and cardiovascular development remains largely unknown [13,14]. In this study, we therefore collected remodeling myocardium tissue (n=18) and control myocardium tissue (n=22), and detected the expression of the 4 miRNAs in these 2 groups. We found that only the expression level of miR-93

Indexed in: [Current Contents/Clinical Medicine] [SCI Expanded] [ISI Alerting System] [ISI Journals Master List] [Index Medicus/MEDLINE] [EMBASE/Excerpta Medica] [Chemical Abstracts/CAS] [Index Copernicus]

was different in the remodeling myocardium tissue, and others are comparable (Figure 1).

miR-93 participates in progressions of several carcinomas. MiR-93 has been reported to serve as a suppressor or promoter in different malignancies [15,16], but it remains unclear how miR-93 function in LVH pathogenesis. It has been shown that there is lower expression of miR-93 in colorectal carcinoma cell lines and human colon cancer tissue than in that of normal colon tissue [17]. Increased miR-93 expression in colon cancer cells suppresses colon cancer proliferation, migration, and invasion [18]. The Wnt/β-catenin pathway was suppressed by miR-93, which was verified by measuring the expression level of cyclin-D1, c-Myc, axin, and β-catenin in this pathway [19,20]. A previous expression analysis suggested downregulation of miR-93 occurs in human malignancies. Nonetheless, further investigation is needed to clarify the clear mechanism and functional role miR-93 in colon cancer. Recent research suggests downregulation of miR-93 protein in colon cancer, indicating that miR-93 may serve as a tumor suppressor in the carcinogenesis of these malignancies [21]. To confirm the regulatory relationship between miR-93 and CCND1, we performed luciferase assay and found that only the luciferase activity from the cells cotransfected with miR-93 and wild-type CCND1 3'UTR was decreased significantly (Figure 4), while cells cotransfected with miR-93 and mutant CCND1 3'UTR were comparable to scramble control (Figure 4). We then analyzed the correlation between the expression level of miR-93 and CCND1 mRNA among the tissues (n=40). which showed a negative regulatory relationship (Figure 5). These findings further confirm that CCND1 is a direct target of miR-93 in HL-1 cells.

CCND1 is commonly known as a human oncogene involved in overexpression and amplification of CCND1; it has been found in oral squamous cell carcinomas, melanoma, lung cancer, and breast cancer. CCND1 overexpression in the mammary gland promotes mammary adenocarcinoma and hyperplasia and amplification of the same gene in stratified squamous epithelium in the esophagus and tongue promotes dysplasia and proliferation [22]. Over amplification of CCND1 reduces serum dependency, reduces cell size, and shortens the G1 phase duration of rodent fibroblasts [23,24]. Cyclin Ds (D3, D2, and D1) activate CDK6 and CDK4, and activation of CDK6 or CDK4 phosphorylates Rb family proteins (retinoblastoma protein: p110, p130 and pRb) [25–27], leading to release of E2F transcription factors. This results in activation of E2f-responsive genes (e.g., cyclin A and cyclin E), which play an important part in DNA synthesis, which further activates CDK2 to promote phosphorylation of pRb. Rb-associated p107 and p130 are known to be crucial in the proliferation of chondrocytes because p107/p130/double-knockout mice presented retarded maturation of chondrocytes and enhanced proliferation of chondrocytes. Inhibition of Mdm2 and activation of Arf triggered the function of p53 in regulating cell apoptosis and cell cycle arrest [28,29]. In the process of apoptosis, Puma, Noxa, and Bax regulated by p53 promote the release of cytochrome C from the mitochondria into the cytoplasm [30]. The apoptosis found in K6H/D1H mice was almost totally rescued by the disruption of p53 [31]. Consequently, as an important factor in the cell cycle checkpoint, p53 is likely to promote apoptosis in response to cell cycle changes induced by overexpression of Ccnd1 and Cdk6 in chondrocytes. A viral homolog of cyclin D1, named K cyclin or viral cyclin (v-cyclin), which is encoded by Kaposi's sarcoma-associated herpesvirus (KSHV), is closely related to CDK6 [32]. In this study, we found that HL-1 cells transfected with miR-93 mimics (50 nM) showed evidently downregulated viability (Figure 7A) when compared with the scramble controls, while cells transfected with (100 nM) and CCND1 siRNA (100 nM) showed even lower viability, indicating that miR-93 reduced the viability of HL-1 cells, while CCND1 enhanced the viability of HL-1 cells. Simultaneously, we also investigated the relative viability of HL-1 cells when transfected with scramble control, miR-93 mimics (50 nM), miR-93 mimics (100 nM), and CCND1 siRNA (100 nM). Cells transfected with miR-93 mimics (50 nM) showed evidently downregulated viability (Figure 7A) when compared with the scramble controls, while cells transfected with (100 nM) and CCND1 siRNA (100 nM) showed even lower viability, indicating that miR-93 reduced the viability of HL-1 cells, while CCND1 enhanced the viability of HL-1 cells.

Conclusions

We found that the downregulation of miR-93 and corresponding upregulation of its direct target gene, CCND1, is responsible for the abnormally enhanced proliferation of cardiomyocytes, and is functionally involved in the pathogenesis of LVH.

Conflict of interest

None.

References:

1. Levy D, Garrison RJ, Savage DD et al: Prognostic implications of echocardiographically determined left ventricular mass in the Framingham Heart Study. N Engl J Med, 1990; 322(22): 1561–66

2. Lauer MS, Anderson KM, Levy D: Influence of contemporary versus 30-year blood pressure levels on left ventricular mass and geometry: The Framingham Heart Study. J Am Coll Cardiol, 1991; 18(5): 1287–94

Indexed in: [Current Contents/Clinical Medicine] [SCI Expanded] [ISI Alerting System] [ISI Journals Master List] [Index Medicus/MEDLINE] [EMBASE/Excerpta Medica] [Chemical Abstracts/CAS] [Index Copernicus]

3. Bauwens FR, Duprez DA, De Buyzere ML et al: Influence of the arterial blood pressure and nonhemodynamic factors on left ventricular hypertrophy in moderate essential hypertension. Am J Cardiol, 1991; 68(9): 925–29
4. Boley E, Pickering TG, James GD et al: Relations of ambulatory blood pressure level and variability to left ventricular and arterial function and to left ventricular mass in normotensive and hypertensive adults. Blood Press Monit, 1997; 2(6): 323–31
5. Cohn JN, Ferrari R, Sharpe N: Cardiac remodeling – concepts and clinical implications: A consensus paper from an international forum on cardiac remodeling. Behalf of an International Forum on Cardiac Remodeling. J Am Coll Cardiol, 2000; 35(3): 569–82
6. Chandrashekhar Y: Role of apoptosis in ventricular remodeling. Curr Heart Fail Rep, 2005; 2(1): 18–22
7. Abbate A, Biondi-Zoccai GG, Baldi A: Pathophysiologic role of myocardial apoptosis in postinfarction left ventricular remodeling. J Cell Physiol, 2002; 193(2): 145–53
8. Ibe W, Sarasti A, Linderman S et al: Cardiomyocyte apoptosis is related to left ventricular dysfunction and remodeling in dilated cardiomyopathy, but is not affected by growth hormone treatment. Eur J Heart Fail, 2007; 9(2): 160–67
9. Abbate A, Biondi-Zoccai GG, Bussani R et al: Increased myocardial apoptosis in patients with unfavorable left ventricular remodeling and early symptomatic postinfarction heart failure. J Am Coll Cardiol, 2003; 41(5): 753–60
10. Sayed D, Hong C, Chen IY et al: MicroRNAs play an essential role in the development of cardiac hypertrophy. Circ Res, 2007; 100(3): 416–24
11. Ruetten H, Dimmeler S, Gehring D et al: Concentric left ventricular remodeling in endothelial nitric oxide synthase knockout mice by chronic pressure overload. Cardiovasc Res, 2005; 66(3): 444–53
12. Wang J, Xu R, Lin F et al: MicroRNA: Novel regulators involved in the remodeling and reverse remodeling of the heart. Cardiology, 2009; 113(2): 81–88
13. Callis TE, Wang DZ: Taking microRNAs to heart. Trends Mol Med, 2008; 14(6): 254–60
14. Cordes KR, Srivastava D: MicroRNA regulation of cardiovascular development. Circ Res, 2009; 104(6): 724–32
15. Hwang HW, Mendell JT: MicroRNAs in cell proliferation, cell death, and tumorigenesis. Br J Cancer, 2006; 94(6): 776–80
16. Bienertova-Vasku J, Mazanek P, Hezova R et al: Extension of microRNA expression pattern associated with high-risk neuroblastoma. Tumour Biol, 2013; 34(4): 2315–19
17. Tang Q, Zou Z, Zou C et al: MicroRNA-93 suppress colorectal cancer development via Wnt/beta-catenin pathway downregulating. Tumour Biol, 2015; 36(3): 1701–10
18. Yang IP, Tsai HL, Hou MF et al: MicroRNA-93 inhibits tumor growth and early relapse of human colorectal cancer by affecting genes involved in the cell cycle. Carcinogenesis, 2012; 33(8): 1522–30
19. Morin PJ, Sparks AB, Korinek V et al: Activation of beta-catenin-Tcf signaling in colon cancer by mutations in beta-catenin or APC. Science, 1997; 275(5307): 1787–90
20. Hu X, Li L, Shang M et al: Association between microRNA genetic variants and susceptibility to colorectal cancer in Chinese population. Tumour Biol, 2014; 35(3): 2151–56
21. Brabletz T, Jung A, Hermann K et al: Nuclear overexpression of the oncoprotein beta-catenin in colorectal cancer is localized predominantly at the invasion front. Pathol Res Pract, 1998; 194(10): 701–4
22. Musgrove EA, Caldon CE, Barraclough J et al: Cyclin D as a therapeutic target in cancer. Nat Rev Cancer, 2011; 11(8): 558–72
23. Wang TC, Cardiff RD, Zukerberg L et al: Mammary hyperplasia and carcinoma in MMTV-cyclin D1 transgenic mice. Nature, 1994; 369(6482): 669–71
24. Mueller A, Odze R, Jenkins TD et al: A transgenic mouse model with cyclin D1 overexpression results in cell cycle, epidermal growth factor receptor, and p53 abnormalities. Cancer Res, 1997; 57(24): 5542–49
25. Resnitzky D, Gossen M, Bujard H, Reed SI: Acceleration of the G1/S phase transition by expression of cyclins D1 and E with an inducible system. Mol Cell Biol, 1994; 14(3): 1669–79
26. Quelle DE, Ashmun RA, Shurtleff SA et al: Overexpression of mouse D-type cyclins accelerates G1 phase in rodent fibroblasts. Genes Dev, 1993; 7(8): 1559–71
27. Jiang W, Kahn SM, Zhou P et al: Overexpression of cyclin D1 in rat fibroblasts causes abnormalities in growth control, cell cycle progression and gene expression. Oncogene, 1993; 8(12): 3447–57
28. Cobrinik D, Lee MH, Hannon G et al: Shared role of the pRB-related p130 and p107 proteins in limb development. Genes Dev, 1996; 10(13): 1633–44
29. Rossi F, MacLean HE, Yuan W et al: p107 and p130 Coordinately regulate proliferation, Cbfa1 expression, and hypertrophic differentiation during endochondral bone development. Dev Biol, 2002; 247(2): 271–85
30. Lowe SW, Sherr CJ: Tumor suppression by Ink4a-Arf: Progress and puzzles. Curr Opin Genet Dev, 2003; 13(1): 77–83
31. Harris SL, Levine AJ: The p53 pathway: Positive and negative feedback loops. Oncogene, 2005; 24(17): 2899–908
32. Li M, Lee H, Yoon DW et al: Kaposi's sarcoma-associated herpesvirus encodes a functional cyclin. J Virol, 1997, 71(3): 1984–91

Indexed in: [Current Contents/Clinical Medicine] [SCI Expanded] [ISI Alerting System] [ISI Journals Master List] [Index Medicus/MEDLINE] [EMBASE/Excerpta Medica] [Chemical Abstracts/CAS] [Index Copernicus]